Am J Physiol Lung Cell Mol Physiol
281: L1068–L1077, 2001.

Keratinocyte growth factor reduces alveolar epithelial susceptibility to in vitro mechanical deformation

JANE OSWARI,[1] MICHAEL A. MATTHAY,[2] AND SUSAN S. MARGULIES[1]
[1]*Department of Bioengineering, University of Pennsylvania, Philadelphia, Pennsylvania 19104-6392; and* [2]*Critical Care Medicine, University of California, San Francisco, California 94143-0624*

Received 28 July 2000; accepted in final form 17 July 2001

Oswari, Jane, Michael A. Matthay, and Susan S. Margulies. Keratinocyte growth factor reduces alveolar epithelial susceptibility to in vitro mechanical deformation. *Am J Physiol Lung Cell Mol Physiol* 281: L1068–L1077, 2001.—Keratinocyte growth factor (KGF) is a potent mitogen that prevents lung epithelial injury in vivo. We hypothesized that KGF treatment reduces ventilator-induced lung injury by increasing the alveolar epithelial tolerance to mechanical strain. We evaluated the effects of in vivo KGF treatment to rats on the response of alveolar type II (ATII) cells to in vitro controlled, uniform deformation. KGF (5 mg/kg) or saline (no-treatment control) was instilled intratracheally in rats, and ATII cells were isolated 48 h later. After 24 h in culture, both cell groups were exposed to 1 h of continuous cyclic strain (25% change in surface area); undeformed wells were included as controls. Cytotoxicity was evaluated quantitatively with fluorescent immunocytochemistry. There was >1% cell death in undeformed KGF-treated and control groups. KGF pretreatment significantly reduced deformation-related cell mortality to only 2.2 ± 1.3% (SD) from 49 ± 5.5% in control wells ($P < 0.001$). Effects of extracellular matrix, actin cytoskeleton, and phenotype of KGF-treated and control cells were examined. The large reduction in deformation-induced cell death demonstrates that KGF protects ATII cells by increasing their strain tolerance and supports KGF treatment as a potential preventative measure for ventilator-induced lung injury.

acute lung injury; barotrauma; mechanical ventilation; mechanotransduction

MECHANICAL VENTILATION is used to care for patients with acute respiratory failure. Although this treatment provides ventilatory support, it can worsen lung injury (5, 37). The effects of high pressures and excessive regional lung volumes can result in life-threatening barotrauma or ventilator-induced lung injury (VILI) (27). Potential mechanisms involved in the onset of VILI have included repeated collapse and reopening of the airspaces (30), inflammation and neutrophil influx (18), and surfactant inactivation (39). Numerous animal studies in the last decade (6, 11, 12, 19, 23, 25, 34) have shown that ventilation with high volumes or airway pressures can induce air leaks, compromise the blood-gas barrier, cause alveolar cell dysfunction, and increase pulmonary edema as well as reduce fluid clearance. Alveolar epithelial injury alone can potentiate pulmonary edema formation even in the presence of normal pulmonary microvascular pressure, plasma oncotic pressure, and endothelial permeability (17).

The recent positive results from the National Institutes of Health-sponsored ventilator management study conducted by the Acute Respiratory Distress Syndrome Network demonstrated that mechanical ventilation with a low tidal volume (6 ml/kg predicted body wt) and a plateau pressure limit (<30 cmH_2O) reduced patient mortality by 22% compared with a traditional tidal volume (12 ml/kg) (5). These findings emphasize the value of experimental models to determine the mechanisms that make the epithelium susceptible to mechanical deformation and to define interventions that protect the epithelium against mechanical deformation. In a previous publication, Tschumperlin et al. (33) examined the relative effects of deformation frequency, duration, and amplitude on cell viability in vitro (33). Cellular injury seemed to occur rapidly, specifically in the first 5 min of cyclic deformation. Deformation-induced injury increased with the frequency of sustained cyclic deformations but was not dependent on the strain rate during a single deformation. When the amplitude of deformation was reduced by superimposing small cyclic deformations on a tonic deformation, cell death was significantly reduced compared with large amplitude deformations with the same peak deformation. This evidence supports the recently published Acute Respiratory Distress Syndrome Network data (5) stating that ventilation with lower tidal volumes but significantly higher positive end-expiratory pressures resulted in lower mortality rates than traditional tidal volume ventilation. These clinical studies confirm the importance of in vitro models in helping to determine the etiology of VILI and develop new therapies for the prevention and treatment of VILI.

After injury to the alveolar epithelium, alveolar type II (ATII) cells proliferate in vivo and eventually differentiate into type I (ATI) cells that line the alveolar epithelium to restore the parenchymal structure (21).

Address for reprint requests and other correspondence: S. S. Margulies, 105 Hayden Hall, Dept. of Bioengineering, Univ. of Pennsylvania, 3320 Smith Walk, Philadelphia, PA 19104-6392 (E-mail: margulies@seas.upenn.edu).

The costs of publication of this article were defrayed in part by the payment of page charges. The article must therefore be hereby marked "*advertisement*" in accordance with 18 U.S.C. Section 1734 solely to indicate this fact.

Keratinocyte growth factor (KGF) is a known potent mitogen of ATII cells after treatment in vivo (14, 24, 35, 36), suggesting a role for KGF in the repair of the alveolar epithelium after lung injury. KGF may also enhance alveolar fluid clearance after acute lung injury by upregulating sodium pump expression and transepithelial sodium transport across the alveolar epithelium (2). It has also been shown to induce an increase in mRNA expression of surfactant protein (SP) A and SP-B after their addition to ATII cells in culture (29), demonstrating a potential role in reversing surfactant dysfunction. KGF can also accelerate wound closure in airway epithelium during cyclic mechanical strain (38) and thus may also enhance epithelial recovery after VILI. Recent evidence (42) demonstrated that KGF pretreatment reduced edema during ex vivo inflations at large tidal volumes. These studies have directed us to evaluate the role of KGF treatment in vivo on the prevention of VILI by measuring the viability of treated and untreated ATII cells exposed to controlled mechanical deformations approximately equivalent to those experienced during large tidal volumes. Previous work by Tschumperlin and Margulies (31) demonstrated the vulnerability of untreated alveolar epithelial cells to deformation 1 and 5 days after isolation. Increasing deformation amplitude was associated with an increasing proportion of nonviable cells after 1 h of cyclic deformation. Untreated cells were most vulnerable after 1 day in culture, but by 5 days, their tolerance to strain had increased significantly. We hypothesized that the specific mechanism involved in the increased tolerance of untreated cells by *day 5* may yield insight into developing new modalities to prevent VILI.

Therefore, the purpose of this study was to measure the role KGF can play in altering the vulnerability of the alveolar epithelium to mechanical deformation and to identify the potential contributions of extracellular matrix (ECM) composition, the actin cytoskeleton, and the phenotype of the alveolar epithelium. Our objective was to determine whether KGF may serve as a cytoprotective strategy as evidenced by enhanced epithelial tolerance to mechanical deformation in vitro.

MATERIALS AND METHODS

Experimental matrix. The experimental matrix consisted of three integrated studies. In the first study, ATII cells seeded on fibronectin-coated elastic membranes were harvested 48 h after instillation with KGF or saline vehicle; after 24 h in culture, they were biaxially strained cyclically in a continuous manner. Cell viability was examined in biaxially strained and in undeformed wells to determine whether KGF instillation enhanced alveolar epithelial resistance to deformation. Comparison with the data in the previously published study by Tschumperlin and Margulies (31) in untreated ATII cells after 1 or 5 days in culture demonstrated no effect due to the saline vehicle, and the remaining untreated control groups in our study consisted of animals receiving no instillation. To examine the specific contribution of the ECM to the cellular response to biaxial strain, in the second study, untreated cells were seeded on ECM obtained from treated cells or untreated cells after 5 days in culture, and their viability, cytoskeleton (F-actin), and phenotype were compared with treated and untreated cells seeded on fibronectin. In the third study, the distinct phenotype and cytoskeleton of treated cells were characterized and compared with those of untreated cells at 1 and 5 days and then correlated with the viability data to evaluate these factors as potential contributors to the cellular deformation tolerance of KGF-treated cells.

KGF or saline instillation. Ten male Sprague-Dawley rats (Charles River, Wilmington, MA) weighing 140–160 g were anesthetized with methoxyfluorane (Mallinckrodt Veterinary, Mundelein, IL). Seven rats received a single intratracheal injection of KGF (5 mg/kg body wt in 0.4 ml of saline plus 0.6 ml of air) and three rats served as controls, receiving a single intratracheal injection of saline alone (0.4 ml plus 0.6 ml of air). ATII cells were isolated 48 h after instillation. Recombinant KGF was generously provided by Dr. Michael Matthay's laboratory (University of California, San Francisco) in collaboration with Amgen (Thousand Oaks, CA). Seven rats that received no intratracheal instillation were used as additional controls for ECM, phenotype, and actin studies.

Cell isolation. The animals were anesthetized with pentobarbital sodium (50 mg/kg body wt intraperitoneally). The trachea was cannulated, the lungs were mechanically ventilated, an abdominal aortotomy was performed, and the lungs were perfused via the pulmonary artery to remove blood. The lungs were excised, and the ATII cells were dissociated and isolated with a technique adapted from Dobbs et al. (10). Briefly, the cells were dissociated with elastase (3 U/ml; Worthington Biochemical, Lakewood, NJ) and minced with a tissue chopper. Cell separation was done by filtration through progressively smaller mesh sizes (400, 160, and 37 μm; Crosswire Cloth, Bellmawr, NJ) and then centrifuged for 10 min at 1,000 rpm. The cells were plated on a bacteriological petri dish precoated with rat IgG (3 mg in 5 ml of Tris·HCl; Sigma, St. Louis, MO). After a 1-h incubation at 37°C in 5% CO_2, the ATII cells were isolated from the macrophages and contaminating cells by gentle panning (10). ATII cell yield was usually doubled 48 h after KGF instillation compared with that in untreated animals, indicating the mitogenic effect of KGF.

Cell culture. ATII cells were resuspended in DMEM supplemented with 10% fetal bovine serum, 25 μg/ml of gentamicin (GIBCO BRL, Life Technologies, Grand Island, NY), and 0.25 μg/ml of amphotericin B (Sigma). For all conditions, the cells were plated at a density of 1.0×10^6 cells/cm^2 on Silastic membranes (Specialty Manufacturing, Saginaw, MI) mounted into our custom-made wells with O-rings (31). Cell attachment was limited to the central portion of each membrane by placing a piece of Tygon tubing (~1-cm diameter) in the center of each well and seeding cells only within this restricted area. This region was coated with fibronectin (40 μg/ml; Boehringer Mannheim Biochemicals, Indianapolis, IN) to assist cell attachment. Cell purity, assessed by phosphine 3R staining of adherent cells after 24 h in culture, was >95% (22). The cells were studied after 24 h in culture.

Cell deformation. After 24 h in culture, eight wells from every isolation were washed with serum-free DMEM supplemented with 1% penicillin (1,000 U/ml) and streptomycin (10 mg/ml; GIBCO BRL), in which sodium bicarbonate was replaced with 20 mM HEPES. Four of the wells were mounted in a custom-designed cell-stretching device previously described and validated (31). The wells were biaxially strained at 25% change in surface area (ΔSA) for 1 h at 15 cycles/min, equivalent to inflation to ~80% of total lung capacity (32). Four no-stretch control wells from each isolation were main-

tained within the device during the experimental period. Experiments were carried out at 37°C in room air. After deformation, three of the strained wells were tested for viability and one was fixed for F-actin analysis. For the unstrained control wells, two were used to test viability and two were fixed for phenotypic characterization. These studies included 24-h cells from the KGF instillation, 24-h untreated cells on KGF ECM, and 24-h untreated cells on *day 5* matrix. All viability data are reported as percent dead cells normalized by unstrained control cells.

Cell viability. Before cellular deformation, ethidium homodimer-1 and calcein-AM (LIVE/DEAD kit, Molecular Probes) were added to the cells at a final concentration of 0.23 and 0.12 μM, respectively. Ethidium homodimer-1 (excitation ~495 nm and emission ~635 nm), which is excluded by the intact plasma membrane of live cells, enters cells with damaged membranes and undergoes a fluorescence enhancement on binding to nucleic acids. Calcein-AM (excitation ~495 nm and emission ~515 nm), a cell-permeant dye, is retained within live cells. One hour after the onset of biaxial strain, control and deformed wells were examined with an inverted epifluorescence microscope (×20 objective, TE-300, Nikon), and images of the cells were captured with a digital imaging system (Hammamatsu, Metamorph 3.0 software, Universal Imaging). Images were acquired from three random locations in the well at both emissions for visualizing ethidium homodimer-1 and calcein-AM (Fig. 1). These images were subsequently analyzed by counting stained cells, and nonviable cells are reported as a percentage of the total number of cells. Results across all wells in an experimental group were averaged and are expressed as means ± SD. Comparisons between specific experimental groups were evaluated with unpaired Student's and Welch's approximate *t*-tests.

Phenotype. To determine whether the phenotype of the cells was related to their response to biaxial strain, two complementary phenotypic markers were evaluated in unstrained cells from every experimental group. Cells from two to four isolations in each group were evaluated for each marker. The phenotype of isolated alveolar epithelial cells was examined at isolation (*day 0*) and on *day 1* (24 h in culture) and compared with the phenotype evaluated in untreated cells maintained in culture for 5 days. *Day 0* cells were cytospun onto slides for immunocytochemistry. *Day 1* and *day 5* cells were stained in our custom-made wells. Specifically, we used an ATI cell-specific monoclonal antibody to RTI_{40} and an ATII-specific polyclonal antibody to proSP-C. RTI_{40} (antibody was a gift from Dr. L. Dobbs, University of California, San Francisco) is a 40- to 42-kDa protein that is specific in the lung to the apical plasma membrane of the rat ATI cell (16). The antibody to proSP-C (a gift from Dr. M. Beers, Children's Hospital of Philadelphia, Philadelphia, PA) labels a precursor of SP-C (1), a lung-specific, hydrophobic peptide found in pulmonary surfactant and synthesized by ATII cells. Although SP-A, SP-B, and SP-D are also made by Clara cells in the lung, SP-C is specific to ATII cells and appears in abundance.

Cells were fixed with 4% paraformaldehyde for 20 min and treated with sodium borohydride (1 mg/ml; Sigma) to reduce endogenous fluorescence. Normal goat serum (GIBCO BRL) was used to block nonspecific sites. Primary antibodies were incubated at room temperature for 1 h. Fluorescein-conjugated and Texas Red-X-conjugated secondary antibodies (Jackson ImmunoResearch Laboratories, West Grove, PA) were incubated at room temperature for 2 h in the dark. Immunofluorescence was preserved with fluorescent mounting medium (DAKO, Carpinteria, CA), and the slides were stored at 4°C.

In our freshly isolated, untreated ATII cells, we confirmed that proSP-C was present in large quantities, whereas RTI_{40} levels were very low, with occasional ATI cells contaminating the isolation as others have found (7). The proportion of positively stained cells was quantified in treated and untreated cells maintained in culture for 1 day, untreated cells maintained in culture for 5 days, and untreated cells seeded onto each ECM material (see *Isolating ECM*) and maintained in culture for 1 day. Images from three randomly selected fields were captured from proSP-C- and RTI_{40}-stained slides (1–3 slides/antibody) in each experimental group as previously described in *Cell viability* for viability analysis. Positively stained cells were counted in each field and are reported as a percentage of the total number of cells in the field. Results across all fields in an experimental group were averaged and are expressed as means ± SD (see Fig. 4). Comparisons between experimental groups were evaluated by Tukey-Kramer test for multiple comparisons.

Isolating ECM. Freshly isolated untreated ATII cells were seeded on the ECM of KGF-instilled cells ($n = 3$ animals) or untreated *day 5* alveolar epithelial cells ($n = 4$ animals). KGF or *day 5* cells were washed with Hanks' balanced salt solution (HBSS) to remove any medium or fetal bovine serum. The cells were then treated with 0.5% Triton X-100 supplemented with 5 mM EDTA for 5 min. The cells were then rinsed off with HBSS three times, leaving behind their ECM. Sterile tubing pieces were then placed over the ECM, and freshly isolated untreated cells were seeded within the center of each well at 1×10^6 cells/cm^2. The cells were incubated for 24 h at 37°C in 5% CO_2.

F-actin. Biaxially strained and undeformed control wells were stained for F-actin with Oregon Green 488 phalloidin (Molecular Probes, Eugene, OR). At least three isolations from each experimental group were used to analyze F-actin distribution. The cells were fixed with 4% paraformaldehyde

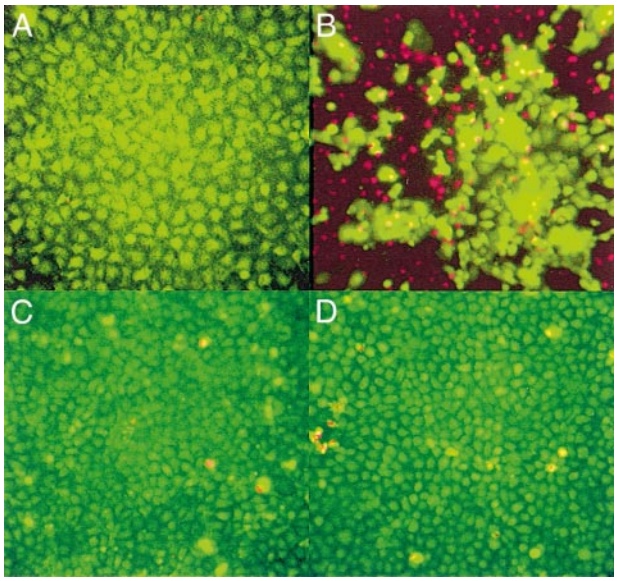

Fig. 1. Enhanced viability after stretch in keratinocyte growth factor (KGF)-treated cells. Cytoplasm of viable cells was stained with calcein-AM (green), and nuclei of nonviable cells were stained with ethidium homodimer-1 (red). *A*: saline vehicle-treated unstretched cells. *B*: saline vehicle-treated cells after 1 h of cyclic stretch (25% change in surface area). *C*: KGF-treated unstretched cells. *D*: KGF-treated cells after same 1-h stretch protocol. Data are expressed as no. of nonviable cells per total no. of cells in the field in Fig. 2.

for 20 min. The cell membranes were permeabilized with 0.1% Triton X-100, and 1% BSA (Sigma) was used to block nonspecific sites. Oregon Green 488 phalloidin was diluted to 5 U/ml and incubated with the cells at room temperature for 20 min. The cells were washed with HBSS, mounted onto a slide, and preserved with fluorescent mounting medium (DAKO).

RESULTS

Viability results. KGF significantly reduced the cell death of ATII cells induced by mechanical deformation (Figs. 1 and 2). Strain-induced viability values were obtained by subtracting the viability of paired, time-matched unstrained control cells from the same isolation and experimental group from the viability of the biaxially strained cells. Thus all reported viability data for strain conditions have been normalized by the unstrained control values for that respective experiment. Specifically, after continuous cyclic (15 cycles/min) deformation (25% ΔSA) equivalent to the average deformation of the epithelium during a tidal volume of ~80% of total lung capacity (32) for 1 h, only 2.2 ± 1.3% of KGF-instilled cells were nonviable (n = 15 wells) compared with 49 ± 5.5% nonviable in the saline-treated cells ($P < 0.001$; n = 6 wells). Unstrained control wells for KGF and saline instillation were 0.74 ± 0.9 (n = 10 wells) and 0.99 ± 0.36% (n = 4 wells) nonviable, respectively. Cell death with saline instillation for undeformed (2.2%) and biaxially strained (49%) conditions were not significantly different from the historic findings by Tschumperlin and Margulies (31) without instillation [3.4 ± 0.6% nonviable without deformation (n = 3 wells) and 43.6 ± 6.6% deformed with the identical protocol (n = 7 wells); $P > 0.10$ and > 0.20, respectively], demonstrating that the saline vehicle alone had no effect on cell viability. Consequently, untreated control measurements for ECM, phenotype, and actin evaluation were made with the cells from animals with no saline instillation.

The effect of the ECM on the susceptibility of ATII cells after mechanical deformation was also analyzed. Untreated ATII cells were seeded on the ECM isolated from *day 1* KGF-treated cells or untreated *day 5* cells. After a 1-h biaxial strain at 25% ΔSA, the proportion of

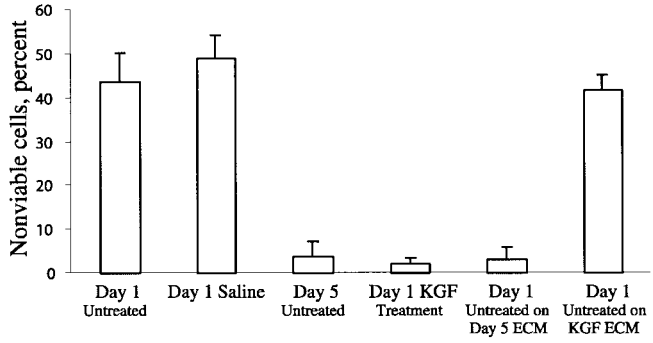

Fig. 2. Proportion of nonviable cells due to 1-h continuous cyclic (15 cycles/min) stretch. ECM, extracellular matrix. Values are means ± SD after values from paired unstretched control wells were subtracted.

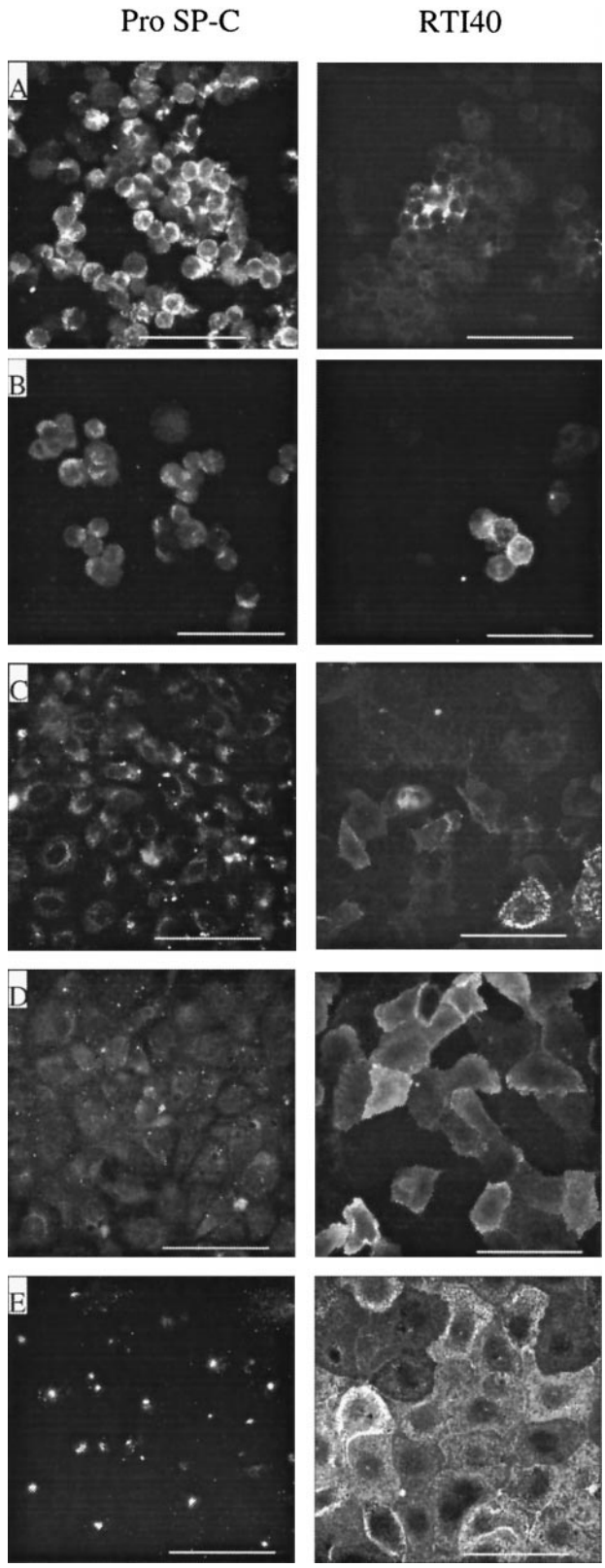

Fig. 3. Influence of time course and KGF on cell phenotype. *A*: untreated, freshly isolated (*day 0*) cells. *B*: freshly isolated (*day 0*) KGF-treated cells. *C*: untreated, freshly isolated cells after 1 day in culture. *D*: KGF-treated cells after 1 day in culture. *E*: untreated cells after 5 days in culture. In cell preparations, the precursor to surfactant protein C (proSP-C) was specific to alveolar type II cells and RTI_{40} was specific to alveolar type I cells. Bars, 50 μm.

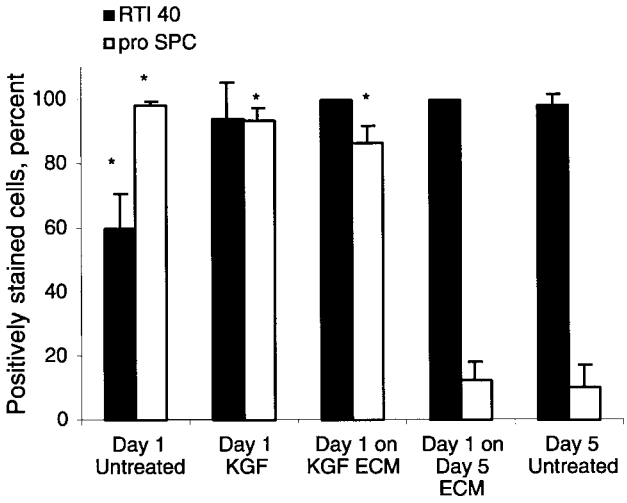

Fig. 4. Proportion of cells expressing type II (proSP-C) or type I (RTI_{40}) phenotype due to 1-h continuous cyclic (15 cycles/min) stretch. Values are means ± SD. Significantly different ($P < 0.05$) from: **day 5* untreated cells; †*day 1* untreated cells. Compare with Figs. 3 and 5.

nonviable ATII cells seeded on *day 5* ECM was significantly reduced to 3.2 ± 2.8% ($n = 11$ wells) compared with ATII cells seeded on fibronectin alone (43.6 ± 6.6% nonviable; $n = 7$ wells). Interestingly, under the same strain conditions, the percent of nonviable ATII cells on KGF-treated ECM was 41.7 ± 3.6 ($n = 7$ wells), not significantly different from untreated cells seeded on fibronectin alone.

Phenotype characterization. Two phenotypic markers were evaluated in unstrained cells from every experimental group with antibodies to RTI_{40} (specific to ATI cells) and proSP-C (specific to ATII cells). Freshly isolated (*day 0*) untreated ATII cells expressed proSP-C strongly but lost this characteristic by *day 5* in culture and, conversely, expressed little RTI_{40} at isolation but showed a progressive increase by *day 5* (Fig. 3). These levels in untreated *day 1* and *day 5* cells were used to establish the extremes of a continuum between type II and type I phenotypes and, as a backdrop, to describe the effect of KGF instillation or ECM on phenotype in our quantitative analysis in Fig. 4.

KGF instillation significantly accelerated the progression of ATII cells to the ATI phenotype, which was at an intermediate phenotype after 24 h in culture. Specifically, the proportion of cells staining positive for RTI_{40} was indistinguishable from that of *day 5* cells, but proSP-C staining still indicated the ATII phenotype of *day 1* cells. These findings are consistent with the hypothesis that loss of the ATII phenotype contributed to the enhanced viability described in Fig. 2 after KGF instillation. To more closely evaluate the potential correlation between phenotype and cell viability, we examined the phenotype of untreated ATII cells on the ECM from KGF-instilled cells (high cell death) and from *day 5* untreated cells (low cell death; see Figs. 4 and 5). The phenotype of both groups, untreated ATII cells on KGF-treated ECM and on *day 5* ECM, was significantly distinct from that of *day 1* untreated cells on a fibronectin matrix as seen in Figs. 4 and 5. Specifically, cells on KGF-treated ECM at an intermediate phase between ATII and ATI phenotypes and cells on *day 5* ECM demonstrate the ATI phenotype in both markers. These results demonstrate that both ECM materials significantly accelerate the phenotype progression from ATII to ATI in culture. Taken together, the viability and phenotype data do not support the hypothesis that an intermediate phenotype confers deformation resistance to the cells.

F-actin distribution. Between *day 1* and *day 5* in culture, untreated cells showed a marked change in their actin distribution. Long stress fibers and a subcortical peripheral actin band around the cell were

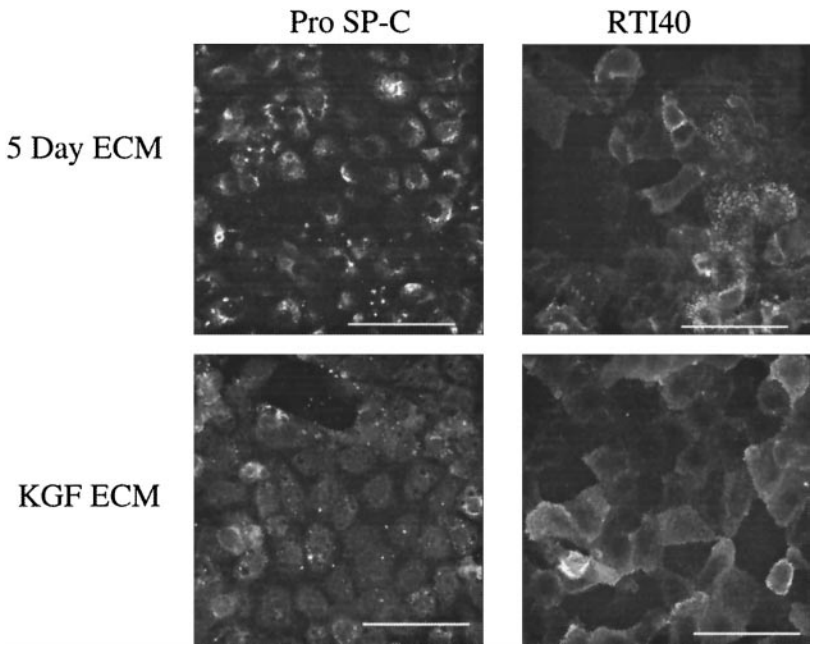

Fig. 5. Influence of ECM on cell phenotype. *Top*: untreated cells were seeded on ECM obtained from untreated cells, maintained for 5 days in culture, and examined after 1 day in culture. *Bottom*: untreated cells were seeded on ECM obtained from cells harvested from KGF-treated animals, maintained in culture for 1 day, and examined after 1 day in culture. Compare with Fig. 3. Bars, 50 μm.

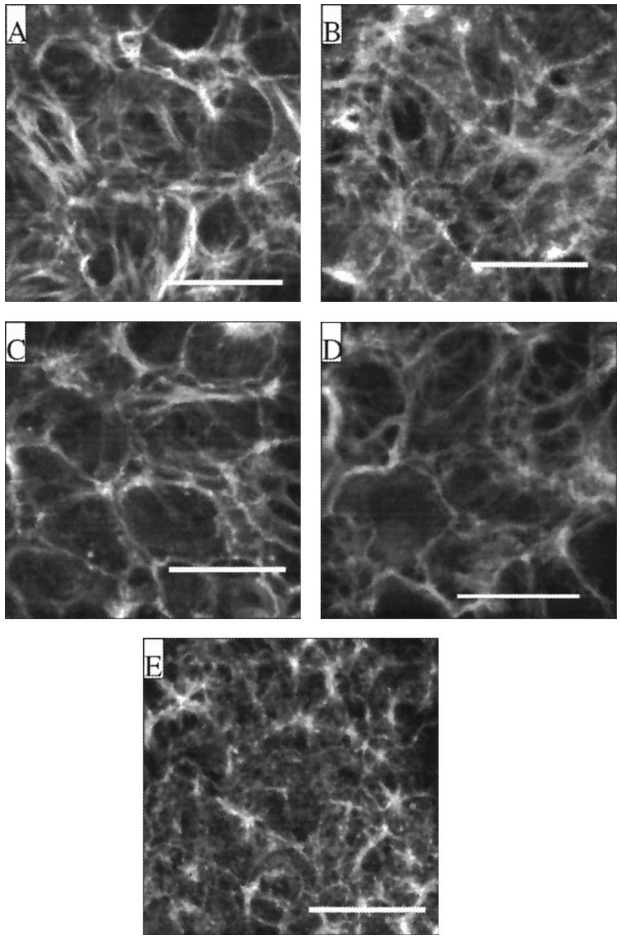

Fig. 6. Influence of time course and KGF on F-actin arrangement. *A* and *C*: unstretched cells. *B* and *D*: after 1 h of cyclic stretch with a 25% change in surface area (15 cycles/min). *A*: untreated cells after 1 day in culture. *B*: KGF-treated cells after 1 day in culture. *C*: untreated cells seeded on KGF-treated ECM after 1 day in culture. *D*: untreated cells seeded on 5-day ECM after 1 day in culture. *E*: untreated cells after 5 days in culture. Cells were stained for F-actin with Oregon Green 488 phalloidin. Bars, 20 μm.

characteristic of *day 1* cells in culture (see Fig. 6*A*). By *day 5* in culture, the cell boundaries were practically indistinguishable due to a loss of the peripheral actin band and the interior fibers were shorter and more networked (see Fig. 6*E*). These cytoskeletal changes observed in untreated cells provided the rationale for determining the actin cytoskeletal distribution in cells after KGF instillation and its potential contribution to enhanced cell viability. After 24 h in culture, cells harvested after KGF instillation showed an actin distribution somewhere between that of *day 1* and *day 5* untreated cells (see Fig. 6*B*). Stress fibers were still evident but shorter, and cell boundaries were less distinct. These results are consistent with our phenotype results, demonstrating that KGF instillation can accelerate the transition toward a type I-like cell.

Because there were distinctive alterations in the actin distribution, we hypothesized that reducing the networked F-actin architecture of KGF-instilled cells with latrunculin A would decrease the tolerance of the cells to mechanical strain. Latrunculin A, an actin-specific agent, sequesters the monomeric G-actin pool, thereby preventing polymerization to F-actin. In a preliminary study, KGF-instilled cells maintained in culture for 1 day were treated with latrunculin A (0.03 μg/ml for 1 h). As anticipated, the actin distribution was focused around the periphery of the cell, with few stress fibers present, thus demonstrating that latrunculin A prevented the formation of F-actin (see Fig. 7). In contrast to our hypothesis, unpaired Student's *t*-test analysis demonstrated that the latrunculin A-treated, KGF-instilled cells showed a very small but significant reduction in cell death (0.12 ± 0.21% nonviable) compared with untreated KGF-instilled cells (2.20 ± 1.25% nonviable; $P = 1.7 \times 10^{-5}$), consistent with enhanced tolerance to mechanical strain when F-actin is reduced. We concluded that it is possible that the enhanced viability of the KGF-treated cells compared with uninstilled control cells may be related to other components of the cytoskeleton such as the intermediate filaments, the microtubules, or a combination of systems.

The F-actin was also analyzed in untreated *day 1* cells on either a KGF-treated ECM or a *day 5* ECM to evaluate the potential correlation between an ATI actin arrangement and enhanced tolerance to deformation. In fact, ATII cells on KGF-treated ECM (with high cell death) had moderate peripheral staining and some stress fibers similar to ATII cells on fibronectin (see Fig. 6*C*). However, in contrast to our hypothesis, cells on *day 5* ECM (with low cell death) also had some stress fibers as well as some peripheral staining (see Fig. 6*D*), also more similar to ATII cells on fibronectin alone than to *day 5* cells.

After 1 h of cyclic biaxial strain at 25% ΔSA, all cell groups experienced similar, pronounced actin cytoskeletal changes: fewer distinct intracellular fibers and more pronounced subcortical peripheral band (see Fig. 8).

To summarize, although ECM may modulate cell viability and phenotype, it does not modulate cytoskel-

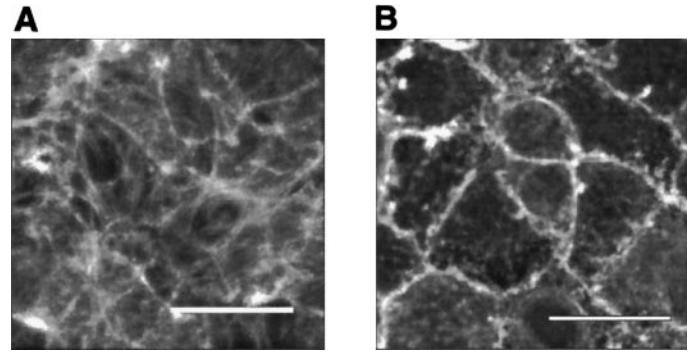

Fig. 7. Alterations in F-actin induced by treatment with latrunculin A. *A*: cells harvested 48 h after in vivo KGF treatment and maintained in culture for 1 day. *B*: cells from the same isolation maintained in culture for 1 day and then treated with latrunculin A (0.03 μg/ml) for 1 h to sequester G-actin and prevent formation of F-actin. Cells were stained for F-actin with Oregon Green 488 phalloidin. Bars, 20 μm.

etal arrangement. However, both cytoskeleton and phenotype data show that KGF instillation hastens the transformation from ATII to ATI characteristics by 24 h in culture.

DISCUSSION

Administration of KGF by intratracheal instillation induces proliferation of alveolar epithelial cells (14, 35, 36) and thus may promote repair of the damaged alveolar epithelium after acute lung injury. Furthermore, KGF instillation has been demonstrated to have a protective effect, reducing pulmonary injury and mortality associated with exposure to bleomycin (28, 45), hyperoxia (24), large tidal volumes (42), and hydrochloric acid instillation (44). These preclinical studies demonstrating that KGF has a cytoprotective effect are consistent with our findings in this study that KGF reduced alveolar epithelial cell death associated with mechanical deformation.

We examined the role of the ECM, cell phenotype, and actin cytoskeleton of alveolar epithelial cells isolated from KGF-treated animals to identify the specific sites responsible for their enhanced tolerance to cyclic equibiaxial distortions. Previous findings by Tschumperlin and Margulies (31) showed that ATII cells maintained in primary culture for 5 days were significantly more tolerant of deformation than after 1 day (Fig. 2). This foundation, coupled with evidence that the ECM components of ATII cells in culture change from entirely fibronectin at 1 day to a composite containing fibronectin, laminin, and trace amounts of type IV collagen by 3 and 6 days in culture (13), led us to hypothesize that the ECM was a major contributing factor to enhanced viability in *day 5* untreated and *day 1* KGF-treated cells (Fig. 2). Freshly isolated cells were seeded on ECM obtained from either *day 5* untreated cells or KGF-treated cells and compared with cells seeded on fibronectin. The results were mixed (Fig. 2); the cells seeded on the ECM of *day 5* cells showed the most rapid phenotypic change and a significant reduction in cell death after deformation, but those on KGF-treated ECM had an intermediate phenotype, with deformation-induced cell death rates that were similar to cells seeded directly on fibronectin. Thus, although the ECM of *day 5* cells seems to correlate with a reduction in deformation-induced cell death, the ECM of treated cells did not contribute to the enhanced tolerance associated with KGF instillation.

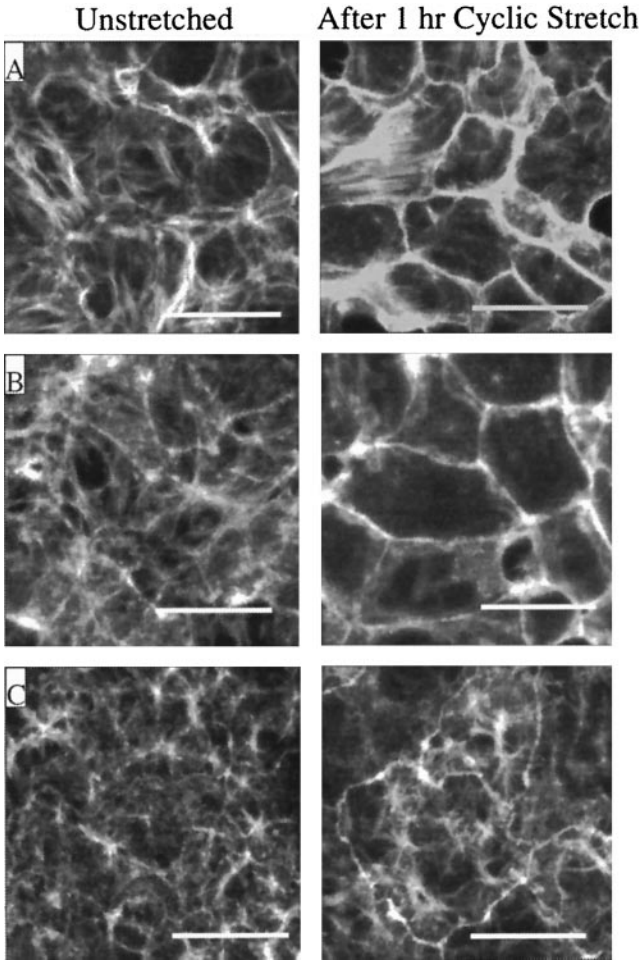

Fig. 8. Influence of continuous cyclic stretch with a 25% change in surface area (15 cycles/min) on F-actin arrangement. *A*: untreated cells after 1 day in culture. *B*: KGF-treated cells after 1 day in culture. *C*: untreated cells after 5 days in culture. Cells were stained for F-actin with Oregon Green 488 phalloidin. Bars, 20 μm.

In untreated cells after isolation, the progression of cell differentiation from type II to type I over days in culture has been well documented (3, 7, 9). To determine the phenotype of the cells, we evaluated two complementary molecular markers in unstrained preparations. As expected, our freshly isolated (*day 0*) and *day 1* untreated ATII cells expressed proSP-C (ATII marker) strongly and lost this characteristic by *day 5* in culture. Conversely, the cells expressed little RTI_{40} (ATI marker) at isolation but showed a progressive increase by *day 5* (Figs. 3 and 4). Projected onto this continuum, we evaluated the relative effect of KGF or alterations in ECM by comparing the RTI_{40} and proSP-C levels on *day 1* in these treatment groups compared with untreated control cells. KGF treatment in vivo accelerates the progression of ATII cells to the ATI phenotype such that by 24 h in culture, their phenotypic alterations are between those for untreated *day 1* and *day 5* cells. Together with the enhanced viability of *day 5* cells, these findings are consistent with the conclusion that the enhanced viability described in Figs. 1 and 2 after KGF instillation is at least partially attributable to the loss of ATII phenotype.

Our results are similar to those of Fehrenbach et al. (14), who demonstrated with immunohistochemistry of lung parenchyma that a single in vivo KGF treatment (5 mg/kg body wt) stimulated cell differentiation from the ATII to the ATI phenotype. Our studies indicate that the in vivo KGF treatment 24 h before cell isolation also causes a more rapid transition in culture to the type I phenotype. In contrast, when cells were exposed after isolation to KGF in vitro from *day 0* or *day 4* in culture to *day 8*, Borok et al. (3) noted decreased expression of aquaporin 5, a water channel

present in freshly isolated ATI cell membranes but not in ATII cells. In untreated cells, aquaporin 5 increased over days in culture, but KGF treatment in vitro inhibited or reversed this temporal progression. Possible explanations for this disparity may include 100,000 times higher KGF concentrations in the instillate and in vivo secondary mediators that were not present during in vitro treatment.

To evaluate the potential correlation between phenotype and cell viability more closely, we examined the phenotype of untreated ATII cells on the ECM from KGF-instilled cells (high cell death) and from *day 5* untreated cells (low cell death; see Figs. 4 and 5). The phenotype of both groups demonstrate ATI-type levels of RTI_{40}, but KGF-treated ECM had transitional levels of proSP-C, whereas *day 5* ECM had progressed to ATI levels of proSP-C as well. Taken together, these results demonstrated that the ECM had a significant effect on the phenotype of these cells after 24 h in culture but that the phenotype of the cells on alternative ECM did not correlate closely with the viability in these groups. Interestingly, after a longer period (72 h) in culture, Lwebuga-Mukasa et al. (20) observed enhanced transformation to an ATI morphology when adult epithelial ATII cells were seeded on human lung basement membrane compared with those on either tissue culture plastic or amnion.

The F-actin cytoskeleton has been linked to transducing external mechanical stimuli and regulating cell function (8, 40) and has been shown to respond to physical forces applied to the cell and be important in cellular resistance to imposed stresses (41). Thus we hypothesized that the F-actin cytoskeletal arrangement may be altered in KGF-treated cells and that this structural change may contribute to the enhanced viability of KGF-instilled cells exposed to biaxial strain. Furthermore, this latter hypothesis was supported by our data demonstrating that untreated cells on *day 1* and *day 5* in culture have specific cytoskeletal arrangements. Specifically, on *day 1*, we observed distinct peripheral bands of actin along with long stress fibers, but by *day 5*, cell boundaries were almost indistinguishable and the actin fibers were shorter and more networked (see Fig. 6). Consistent with this hypothesis, we expected that the actin in the KGF-instilled cells would be similar to that in *day 5* untreated cells. We found that the actin in KGF-instilled cells had stress fibers (characteristic of untreated cells on *day 1*) but also had shorter, more networked actin fibers and a less distinct peripheral band, typical of *day 5* cells. Thus, consistent with the phenotype data, KGF seemed to accelerate the progression of ATII cells to develop ATI cell features but that actin arrangement does not consistently correlate with viability. We conclude that the enhanced viability of the KGF-treated cells may be related to other components of the cytoskeleton such as the intermediate filaments, the microtubules, or a combination of systems.

In addition to Borok et al. (2, 3), other investigators have exposed cells to KGF after isolation in an in vitro setting and have demonstrated a reduction in lung injury due to H_2O_2 and radiation exposure (26, 43) and accelerated repair after epithelial injury (38). For comparative purposes, we conducted a limited investigation to evaluate the viability of alveolar epithelial cells harvested from untreated lungs after in vitro KGF treatment. At the time of seeding the cells onto fibronectin-coated membranes, KGF [0, 10 (2, 3), or 50 (38) ng/ml] was added to the medium. After 1 day in culture, these cells were exposed to the same deformation protocol described in MATERIALS AND METHODS, and the proportion of nonviable cells is expressed relative to unstrained control and untreated control cells (data not shown). There was no significant dose response such that the tolerance of the cells to biaxial strain was not significantly enhanced with the in vitro KGF treatment at either concentration ($P > 0.05$). Thus the dramatic in vivo response, with the lack of an in vitro effect, may be attributed to differences in KGF concentration (as discussed above), shorter exposure time (48-h exposure in vivo vs. 24 h in vitro), or secondary mediator factors present only in vivo. The in vitro treatment time was selected to allow for comparison with all of our formal experimental groups in which the cells were studied after 24 h in culture. Thus we conclude that comparisons between in vivo and in vitro KGF preparations must be made cautiously and that results obtained in an in vitro model should be reconfirmed in vivo before extension to the clinical setting.

The mechanism for the cytoprotective effect on alveolar epithelial cells may relate to changes in the phenotype, ECM components, or the cytoskeleton of ATII cells or to other aspects of the mechanotransduction pathway of the cell. For example, the ECM is closely associated with cytoskeletal mechanotransduction, and integrins (4, 15) transduce forces between the cytoskeleton from the ECM. Our results indicate that by 5 days in culture or after 24 h on *day 5* ECM, cells have an ATI-type phenotype based on two markers, and they develop a significant resistance to deformation-induced death compared with cells after 1 day in culture (31). This phenomenon of increased resistance was also observed after a single instillation of KGF, yet the phenotype of these cells was at an intermediate stage between ATII and ATI. Although the specific mechanism involved is still unknown, we do know that the cytoskeleton and the ECM play a role. Future studies are needed to address these mechanisms and their relationships with each other.

Previously, Tschumperlin and Margulies (31) showed that in vitro cyclic biaxial mechanical deformation causes rapid cell death in ATII cells after 1 day in culture. In this study, we found that a single in vivo treatment with KGF has a dramatic effect in the reduction in cell death from in vitro mechanical deformation. These findings support the potential role of KGF treatment as a protective measure for deformation-induced alveolar epithelial injuries associated with VILI. Finally, this study provides insight into new preventative therapies in addition to a reduction in tidal volume (5) to decrease the high morbidity and

mortality rates related to ventilator-associated lung injury.

We would like to thank Amgen, Incorporated for providing the keratinocyte growth factor, Dr. Yibing Wang for showing us the instillation technique, Dr. Michele Hawk for help with data analysis, Dr. Leland Dobbs and Dr. Michael Beers for generously providing the RTI_{40} and surfactant proprotein C antibodies, respectively, and Dr. Sandra Bates for the use of her laboratory equipment for some of the histological stains.

Support for this work was provided by National Heart, Lung, and Blood Institute Grants R01-HL-57204 and R01-HL-51854 and National Science Foundation Grant BES 9702088.

REFERENCES

1. **Beers MF, Wali A, Eckenhoff MF, Feinstein SI, Fisher JH, and Fisher AB.** An antibody with specificity for surfactant protein C precursors: identification of pro-SP-C in rat lung. *Am J Respir Cell Mol Biol* 7: 368–378, 1992.
2. **Borok Z, Danto SI, Dimen LL, Zhang XL, and Lubman RL.** Na^+-K^+-ATPase expression in alveolar epithelial cells: upregulation of active ion transport by KGF. *Am J Physiol Lung Cell Mol Physiol* 274: L149–L158, 1998.
3. **Borok Z, Lubman RL, Danto SI, Zhang XL, Zabski SM, King LS, Lee DM, Agre P, and Crandall ED.** Keratinocyte growth factor modulates alveolar epithelial cell phenotype in vitro: expression of aquaporin 5. *Am J Respir Cell Mol Biol* 18: 554–561, 1998.
4. **Borradori L and Sonnenberg A.** Structure and function of hemidesmosomes: more than simple adhesion complexes. *J Invest Dermatol* 112: 411–418, 1999.
5. **Brower RG, Matthay MA, Morris A, Schoenfield D, Thompson BT, and Wheeler A.** Ventilation with lower tidal volumes compared with traditional tidal volumes for acute lung injury and the acute respiratory distress syndrome. The Acute Respiratory Distress Syndrome Network. *N Engl J Med* 342: 1301–1308, 2000.
6. **Cilley RE, Wang JY, and Coran AG.** Lung injury by moderate lung overinflation in rats. *J Pediatr Surg* 28: 488–495, 1993.
7. **Danto SI, Zabski SM, and Crandall ED.** Reactivity of alveolar epithelial cells in primary culture with type I cell monoclonal antibodies. *Am J Respir Cell Mol Biol* 6: 296–306, 1992.
8. **Dewey CF Jr.** Effects of fluid flow on living vascular cells. *J Biomech Eng* 106: 31–35, 1984.
9. **Dobbs LG.** Isolation and culture of alveolar type II cells. *Am J Physiol Lung Cell Mol Physiol* 258: L134–L147, 1990.
10. **Dobbs LG, Gonzalez R, and Williams MC.** An improved method for isolating type II cells in high yield and purity. *Am Rev Respir Dis* 134: 141–145, 1986.
11. **Dreyfuss D, Basset G, Soler P, and Saumon G.** Intermittent positive-pressure hyperventilation with high inflation pressures produces pulmonary vascular injury in rats. *Am Rev Respir Dis* 132: 880–884, 1985.
12. **Dreyfuss D, Soler P, Basset G, and Saumon G.** High inflation pressure pulmonary edema. *Am Rev Respir Dis* 137: 1159–1164, 1988.
13. **Dunsmore SE, Martinez-Williams MC, Goodman RA, and Rannels DE.** Composition of extracellular matrix of type II pulmonary epithelial cell sin primary culture. *Am J Physiol Lung Cell Mol Physiol* 269: L754–L765, 1995.
14. **Fehrenbach H, Kasper M, Tschernig T, Pan T, Schuh D, Shannon JM, Muller M, and Mason RJ.** Keratinocyte growth factor-induced hyperplasia of rat alveolar type II cells in vivo is resolved by differentiation into type I cells and by apoptosis. *Eur Respir J* 14: 534–544, 1999.
15. **Green KJ and Jones JCR.** Desmosomes and hemidesmosomes: structure and function of molecular components. *FASEB J* 10: 871–881, 1996.
16. **Gonzalez RF and Dobbs LG.** Purification and analysis of RTI40, a type I alveolar epithelial cell apical membrane protein. *Biochim Biophys Acta* 1429: 208–216, 1998.
17. **Gorin AB and Stewart PA.** Differential permeability of endothelial and epithelial barriers to albumin flux. *J Appl Physiol* 47: 1315–1324, 1979.
18. **Kawano T, Mori S, Cybulsky M, Burger R, Ballin A, Cutz E, and Bryan AC.** Effect of granulocyte depletion in a ventilated surfactant-depleted lung. *J Appl Physiol* 62: 27–33, 1987.
19. **Kolobow T, Moretti MP, Fumagalli R, Mascheroni D, Prato P, Chen V, and Joris M.** Severe impairment in lung function induced by high peak airway pressure during mechanical ventilation. An experimental study. *Am Rev Respir Dis* 135: 312–315, 1987.
20. **Lwebuga-Mukasa JS, Ingbar DH, and Madri JA.** Repopulation of human alveolar matrix by adult rat type II pneumocytes in vitro. A novel system for type II pneumocyte culture. *Exp Cell Res* 162: 423–435, 1986.
21. **Mason RJ and Williams MC.** Alveolar type II cells. In: *The Lung: Scientific Foundations,* edited by Crystal RG and West JB. New York: Raven, 1991, p. 235–246.
22. **Mason RJ, Williams MC, Widdicombe JH, Sanders MJ, Misfeldt DS, and Berry LG Jr.** Transepithelial transport by pulmonary alveolar type II cells in primary culture. *Proc Natl Acad Sci USA* 79: 6033–6037, 1982.
23. **Muscedere JG, Mullen JB, Gan K, and Slutsky AS.** Tidal ventilation at low airway pressure can augment lung injury. *Am J Respir Crit Care Med* 149: 1327–1334, 1994.
24. **Panos RF, Bak PM, Simonet WS, Rubin JS, and Smith LJ.** Intratracheal instillation of keratinocyte growth factor decreases hyperoxia-induced mortality in rats. *J Clin Invest* 96: 2026–2033, 1995.
25. **Parker JC, Townsley MI, Rippe B, Taylor AE, and Thigpen J.** Increased microvascular permeability in dog lungs due to high peak airway pressures. *J Appl Physiol* 57: 1809–1816, 1984.
26. **Savla U and Waters CM.** Barrier function of airway epithelium: effects of radiation and protection by keratinocyte growth factor. *Radiat Res* 150: 195–203, 1998.
27. **Slutsky AS.** Consensus conference on mechanical ventilation. *Intensive Care Med* 20: 150–162, 1994.
28. **Sugahara K, Iyama K, Kuroda MJ, and Sano K.** Double intratracheal instillation of keratinocyte growth factor prevents bleomycin-induced lung fibrosis in rats. *J Pathol* 186: 90–98, 1998.
29. **Sugahara K, Rubin JS, Mason RJ, Aronsen EL, and Shannon JM.** Keratinocyte growth factor increases mRNAs for SP-A and SP-B in adult rat alveolar type II cells in culture. *Am J Physiol Lung Cell Mol Physiol* 269: L344–L350, 1995.
30. **Tremblay L, Valenza F, Ribeiro SP, Li J, and Slutsky AS.** Injurious ventilatory strategies increase cytokines and c-fos mRNA expression in an isolated rat lung model. *J Clin Invest* 99: 944–952, 1997.
31. **Tschumperlin DJ and Margulies SS.** Equibiaxial deformation-induced injury of alveolar epithelial cells in vitro. *Am J Physiol Lung Cell Mol Physiol* 275: L1173–L1183, 1998.
32. **Tschumperlin DJ and Margulies SS.** Alveolar epithelial surface area-volume relationship in isolated rat lungs. *J Appl Physiol* 86: 2026–2033, 1999.
33. **Tschumperlin DJ, Oswari J, and Margulies SS.** Deformation-induced injury of alveolar epithelial cells: effect of frequency, duration, and amplitude. *Am J Respir Crit Care Med* 161: 1–6, 2000.
34. **Tsuno K, Miura K, Takeya M, Kolobow T, and Morioka T.** Histopathologic pulmonary changes from mechanical ventilation at high peak airway pressures. *Am Rev Respir Dis* 143: 1115–1120, 1991.
35. **Ulich TR, Yi ES, Longmuir K, Yin S, Biltz R, Morris CF, Housley RM, and Pierce GF.** Keratinocyte growth factor is a growth factor for type II pneumocytes in vivo. *J Clin Invest* 93: 1298–1306, 1994.
36. **Wang Y, Folkesson HG, Jayr C, Ware LB, and Matthay MA.** Alveolar epithelial fluid transport can be simultaneously upregulated by both KGF and β-agonist therapy. *J Appl Physiol* 87: 1852–1960, 1999.
37. **Ware LB and Matthay MA.** The acute respiratory distress syndrome. *N Engl J Med* 342: 1334–1349, 2000.

38. **Waters CM and Savla U.** KGF accelerates wound closure in airway epithelium during cyclic mechanical strain. *J Cell Physiol* 181: 424–432, 1999.
39. **Webb HH and Tierney DF.** Experimental pulmonary edema due to intermittent positive pressure ventilation with high inflation pressures. Protection by positive end-expiratory pressure. *Am Rev Respir Dis* 110: 556–565, 1974.
40. **Wechezak AR, Viggers RF, and Sauvage LR.** Fibronectin and F-actin redistribution in cultured endothelial cells exposed to shear stress. *Lab Invest* 53: 639–647, 1985.
41. **Wechezak AR, Wight TN, Viggers RF, and Sauvage LR.** Endothelial adherence under shear stress is dependent upon microfilament reorganization. *J Cell Physiol* 139: 136–146, 1989.
42. **Welch DA, Summer WR, Dobard EP, Nelson S, and Mason CM.** Keratinocyte growth factor prevents ventilator-induced lung injury in an ex vivo rat model. *Am J Respir Crit Care Med* 162: 1081–1086, 2000.
43. **Wu KI, Pollack N, Panos RJ, Sporn PH, and Kamp DW.** Keratinocyte growth factor promotes alveolar epithelial cell DNA repair after H_2O_2 exposure. *Am J Physiol Lung Cell Mol Physiol* 275: L780–L787, 1998.
44. **Yano T, Deterding RR, Simonet WS, Shannon JM, and Mason RJ.** Keratinocyte growth factor reduces lung damage due to acid instillation in rats. *Am J Respir Cell Mol Biol* 15: 433–442, 1996.
45. **Yi ES, Salgado M, Williams S, Kim SJ, Masliah E, Yin S, and Ulich TR.** Keratinocyte growth factor decreases pulmonary edema, transforming growth factor-beta and platelet derived growth factor-BB expression, and alveolar type II cell loss in bleomycin-induced lung injury. *Inflammation* 22: 315–325, 1998.